Journal of Theoretical and Applied Mechanics, Sofia, Vol.50 (2020) pp. 114-129
SOLID MECHANICS

DYNAMICS OF CHAINS CONTAINING BI-STABLE ELASTIC ELEMENT AS STABLE NEGATIVE STIFFNESS

AKINTOYE OLUMIDE OYELADE*

Department of Civil and Environmental Engineering, University of Lagos, Akoka, Nigeria

[Received: 26 June 2018. Accepted: 30 April 2020]

ABSTRACT: The instability of negative stiffness materials or systems is rooted in their thermodynamic state, which is not in equilibrium with its environment. In this paper, a model of a chain of masses joined by springs with a non-monotone dependence of the spring force versus spring displacement (negative stiffness) relation is made stable by constraining it in positive matrix. The stability of the system is tested using energy function. Numerical experiments are conducted to test the dynamics of two mass model system under small external excitation. The numerical results are validated for a range of parameters by comparing the predictions with calculations from analytical approximation using Newton Harmonic Balance (NHB) method. The presented results highlight prospects in the design of mechanical metamaterials based on negative-stiffness elements.

KEY WORDS: Bi-stable element, negative stiffness, numerical, stability analysis.

1 INTRODUCTION

It is well known that the study of solitary waves and solitons has proved fruitful in many areas of condensed-matter physics [1]. Special consideration has been given to the dynamics of a one-dimensional chain of masses m connected by identical non-monotonic springs. In such model with a variable potential, there is phase transition of the system; the system goes over from one steady state, when the elongation of each spring is constant, to another steady state, when the masses oscillate with some period [2]. The later phase is called the twinkling phase, which can dissipate energy at a fast rate by transforming kinetic energy into high-frequency oscillations. Furthermore, the dynamic response of non-monotonic force chains has shown theoretically to result in solitary waves [3, 4].

Although the positive effects of bi-stable elements on the performance of mechanical, acoustic and composites is well known [5–7, 9], previous research has focused on avoiding the critical (unstable equilibrium) point. However, dissipating the stored

*Corresponding author e-mail: aoyelade@unilag.edu.ng

energy and making use of the negative stiffness could serve as an interesting ways of introducing negative stiffness, and nonlinear effects into structures, which provides opportunities to improve mechanical and acoustic properties.

An unconstrained, system containing negative stiffness is unstable by itself [10]. In fact, the stability of an externally unconstrained, elastic body requires the positive-definiteness of the elastic stiffness tensor [11]. Therefore, the stability of a general (unconstrained) composite has been theorized to require the positive-definiteness of the elastic properties of each composite constituent. Likewise, the behavior of systems containing conventional and negative stiffness element has been proved to be stable under certain conditions [10–13]. This discovery of way to stabilized negative stiffness has opened up a vast area of research covering several fields of application. For examples, in vibration isolation of mechanical equipment in which the dynamic effective stiffness is reduced to zero at equilibrium point [14, 15]. In biometrics, Nima et al. [16] designed powered hand prosthesis with negative stiffness. A significant amount of stiffness was reduced for the child hand prosthesis, which enhanced its usage. Attary et al. [17] constructed a true negative stiffness member which does not need external power, sensors and controllers to generate the desired forces. The system can be used in new buildings as well as for seismic retrofit.

Negative stiffness elements are elicited via phase transformations when ferroelastic materials undergo microscopic instabilities under temperature controlled [18, 19]. The second class through different magnetic configurations [20, 21], and the last by the use of springs such as bi-stable [22], Euler beam [14], and compressed [23].

However, in most of the generated transient negative stiffness, all have been in parallel with the positive springs in which dynamic stiffness is set equal to zero as in the case of 'zero-stiffness' oscillators. Elena et al. [10] studied a negative linear spring in a positive stiffness but failed to propose a way to achieve the desired load-deflection curve. Oyelade et al. [20] conducted experiments using a 1-D spring-mass system to demonstrate the effect of negative stiffness. Magnetic force was used to produce the linear negative stiffness.

In this paper, we make use of a numerical method to provide an alternative way of creating stable NS within a positive stiffness using bi-stable element.

2 Chains with Positive and Bi-stable Spring Model

If we consider a system of 1-D chain with N springs, as shown in Fig. 1, the potential energy of the system will be

$$\Pi = \frac{1}{2} \sum_{i=1}^{N} \left[k_i \left(x_i - x_{i-1}\right)^2 + k_{i+1} \left(x_{i+1} - x_i\right)^2 \right] . \tag{1}$$

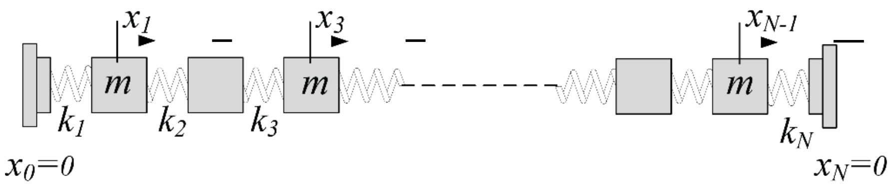

Fig. 1: System of 1-D chain.

The effective stiffness of the spring is

$$\bar{k}^{-1} = \sum_{i=1}^{N} k_i^{-1}\,, \tag{2}$$

and the Hessian Matrix of the second derivatives takes the form

$$H = \begin{vmatrix} k_1+k_2 & -k_2 & & & & \\ -k_2 & k_2+k_3 & & & & \\ & -k_3 & k_3+k_4 & -k_4 & & \\ & & -k_4 & k_4+k_5 & -k_5 & \\ & & & & k_i+k_{i+1} & -k_{i+1} \\ & & & & & k_{N-1}+k_N \end{vmatrix}. \tag{3}$$

Empty spaces denote zero entries. It is well known that for stability $\bar{k} > 0$. The condition for stability also requires

$$D_\Delta > 0\,, \tag{4}$$

where D_Δ is leading principal minor of order Δ of Eq. (3). Therefore, using the two conditions of stability: positive definite of effective stiffness and that of D_Δ, Puglisi and Truskinovsky [2] proved that one of the stiffness of the chain can be negative. Furthermore Elena et al. [10] determined the critical concentration of negative stiffness inclusion in the matrix for stability. Now consider a 3 mass model, which consists of a bi-stable element consisting of one linear elastic spring with stiffness k_0 and two linear springs k as shown in Fig. 2. The springs are positive at the unstressed state. One end of spring k_0 is connected to mass 2 and the other end to mass 3. All joints allow horizontal translation except the end of spring k that is fixed. A horizontal displacement at x_1 will result in horizontal displacement of m_2 and m_3. Hence, we may treat the system as one dimensional in the following. The total Lagrangian of the system gives

$$L\left(x_i,\dot{x}_i\right) = \left(\sum_{i=2}^{3} \frac{m\dot{x}_i^2}{2}\right) - \Pi\left(x_i\right)\,, \tag{5}$$

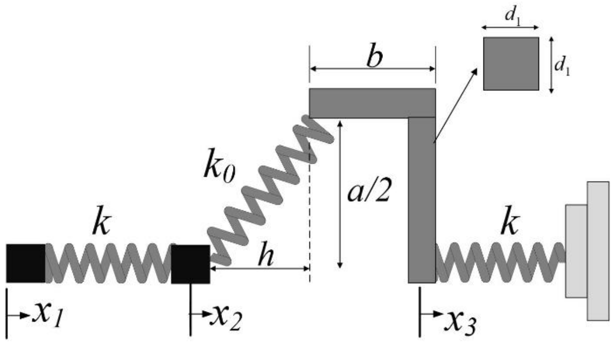

Fig. 2: 1-D mass-spring chain with bi-stable element.

where $\Pi(x_i)$ is the potential energy stored by the structure given by

$$\Pi = \frac{1}{2}k\left[(x_2 - x_1)^2 + x_3^2\right] + \frac{1}{2}k_0\left(\sqrt{\left(\frac{a}{2}\right)^2 + h^2} - \sqrt{\left(\frac{a}{2}\right)^2 + (h + x_3 - x_2)^2}\right)^2 . \tag{6}$$

The rigid body member has the following parameters: $a = 40$ mm, $b = 10$ mm, $h = 20$ mm, $d_1 = 0.5$ mm, $m_2 = 8$ g, $k = 117$ N/m, $E = 1.11$ N/m and $\rho = 1$ g/mm, where a, b, h and d_1 are geometric parameters, while m_2, k, E and ρ are the mass 2, spring stiffness, modulus and density, respectively. The horizontal displacement is defined as $x_i\,(i = 1 - 3)$ We introduce non-dimensional parameters to help study the system without stipulating the stiffness constant and geometry explicitly. We define

$$\kappa_0 = \frac{k_0}{k}\ , \quad \kappa = \frac{k}{k}\ , \quad \delta = \frac{a}{2h}\ , \quad \bar{x}_i = \frac{x_i}{h}\ , \quad [\forall i = 1, 2, 3]\ . \tag{7}$$

The restoring forces of oscillators 2 and 3 can be found by differentiation of Eq. (6), and adding the forces in the springs, which gives

$$F = \begin{cases} F_2 = \dfrac{\kappa_0\,(1 - \bar{x}_2 + \bar{x}_3)\,(\phi - \psi)}{\psi} \\ F_3 = \kappa\,(\bar{x}_3 + \bar{x}_2 - \bar{x}_1) \end{cases} , \tag{8}$$

where $\varphi = \sqrt{\delta^2 + 1}$; $\psi = \sqrt{\delta^2 + \left(1 - 2\bar{x}_2 + \bar{x}_2^2 + 2\bar{x}_3 - 2\bar{x}_2\bar{x}_3 + \bar{x}_3^2\right)}$. For numerical simulation we have the non-dimensional parameters: $\kappa = 1$, $\kappa_0 = 0.256$

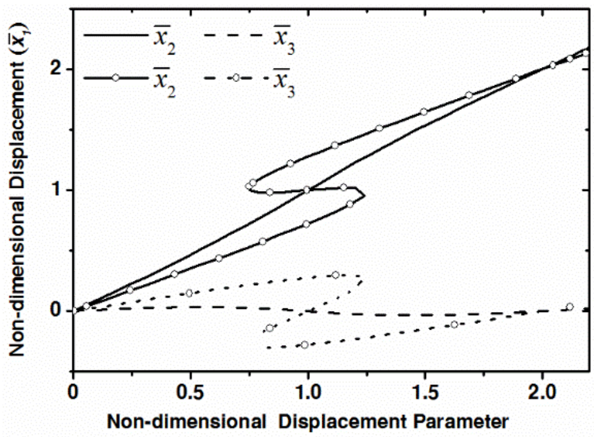

Fig. 3: Equilibrium path of the model for $\delta = 1$, $\kappa_0 = 0.256$ (line) and $\delta = 0.5$, $\kappa_0 = 1$ (line with circle).

and 1.0, $\delta = 1.0$ and 0.5. Generally for static equilibrium path in geometrically non-linear field as we have above, the arch length method [24,25], is appropriate to follow equilibrium paths which offer stable and unstable points. The equilibrium path of the model is plotted in Fig. 3. When the geometric parameter $\delta = 0.5$ and $\kappa_0 = 1.0$ there is a snap through around the midpoint. For $\bar{x}_2$ to be near one and linear, geometry parameter δ has to be chosen carefully. If not, snap through will occur far-off from one, and curve $\bar{x}_2$ becomes non-linear as we have in this case. However, with $\delta = 1.0$ and $\kappa_0 = 0.256$ the compressed spring displayed a linear relationship with the displacement loading. When the dimensional displacement load reaches 0.972, $\bar{x}_2$ has value of 0.968 prior to snap through of the spring.

Retrieving the parameters of the displacements as the system is subjected to displacement loading, the potential energy and force displacement curve is shown in Fig. 4. The potential energy of the system is found to exhibit a double well energy form with two stable points at $\bar{x}_1 = 0$, $\bar{x}_2 = 2$ and a 'forbidden' region in between this range. This demonstrates characteristics of a bi-stable element. Consequently, the overall energy-displacement relations take the following form:

$$\Pi(\bar{x}_1) = \begin{cases} \Pi_1(\bar{x}_1) & \text{if } \bar{x}_1 \leq \mathrm{M} \\ \Pi_2(\bar{x}_1) & \text{if } \mathrm{M} \leq \bar{x}_1 \leq \mathrm{N} \\ \Pi_3(\bar{x}_1) & \text{if } \bar{x}_1 \geq \mathrm{N} \end{cases}, \tag{9}$$

where M and N are the borders of non-convexity of the potential energy of the system. The maximum position of non-convexity corresponds to points of zero force in force

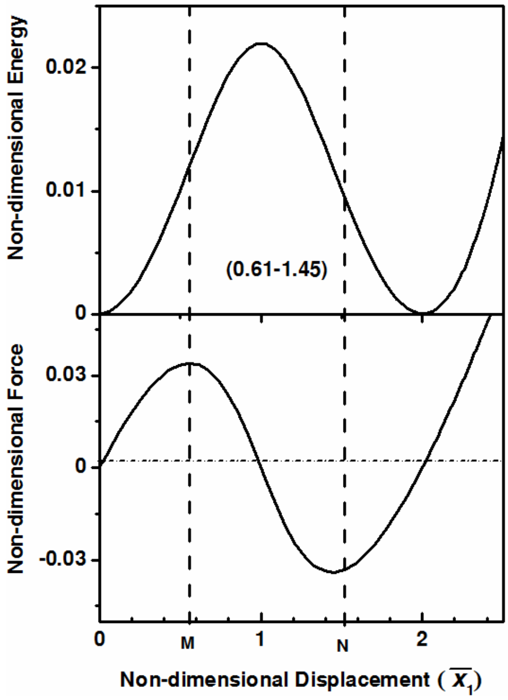

Fig. 4: Total Non-dimensional Energy and Non-dimensional Force Displacement of the system.

displacement diagram. The restoring force in the oscillator two is a non-monotonic bi-stable function of displacement as shown in Fig. 4.

We are interested in the position where $x_2 = 1$. Though this position is not on equilibrium path – Fig. 3 ($\delta = 1$, $\kappa_0 = 0.256$). However, the nearest position before snap through is 0.968, and our interest is investigating the stability of this position for constrained and unconstrained systems.

2.1 System stability

In general, we can broadly distinguish methods of stability analysis in dynamics systems into analysis of equation of motion and energy landscape method. The former provides unique ways of handling stability of nonlinear or even non-autonomous dynamical systems. This is made possible by combining the concept of energy considerations and that of equilibria of differential equations. For dissipative systems such as viscoelastic, Wang et al. [26] used this method in determining the stability of negative stiffness in viscoelastic material. The eigenvalues of perturbed systems is investigated under Lyapunov's theorem. Energy method is based on the second law of thermodynamics, which stipulates that for any isolated system undergoing a thermodynamic process, the infinitesimal change in entropy will always be positive. For equilibrium of isolated system, Gibbs concluded that its variation energy should either vanish or be positive. This means that the strain energy function is positive definite. This outcome is imperative for the present work as it gives a relationship between the strain energy of the system, which is related to its stiffness. Therefore, for stability of a system, the determinant of the Hessian matrix of the energy equation should be positive

$$H_{i,j} = \left| \frac{\partial^2 \Pi}{\partial x_i \partial x_j} \right| \geq 0 \,. \tag{10}$$

2.2 Stability of unconstrained and constrained models

Points M and N in Fig. 4 are regions of negative stiffness or positions where the slope of the force displacement changes to negative. The points have value of 0.55 and 1.55 respectively at $\bar{x}_2$. As expected, instability using Eq. (10) occurs exactly at the same points as shown in Fig. 5, where the stability of the unconstrained is plotted against $\bar{x}_2$. As the model is loaded from point $\bar{x}_1$ the system becomes unstable when $\bar{x}_2$ equals 0.55. This is as a result of change in the value of inclined spring stiffness from positive to negative value. The reduction is due to inclination of spring k_0. The reduction in stiffness makes the spring to store energy inside the spring as it moves along $\bar{x}_2$. Therefore we have the maximum energy stored at minimum stiffness. When the dimensionless stiffness k_0 becomes negative at point 0.58, the system becomes unstable Fig. 5.

However, if the system is constrained at position $\bar{x}_1$ at interval along the equilibrium path, the system becomes stable even at $\bar{x}_2$ equal 0.968. This is revealed in Fig. 5 where Eq. (10) is positive definite for all displacement $\bar{x}_1$. This clearly shows that for the selected configuration, negative stiffness generated is stable within the positive stiffness matrix under constrain. In the next session, numerical analysis is performed for the constrained at the position of minimum negative stiffness where $\bar{x}_2$ equals 0.968. The minimum negative dimensionless stiffness generated at this position is -0.106.

3 Numerical and Analytical Investigations

The behavior of vibration in linear and nonlinear mechanical systems has been extensively studied [20, 27, 28]. Generally the non-linearity could be of a cubic, quadratic, and sometimes a complex function. In our model, the restoring forces on oscillator two are approximately as a linear since we are interested in small displacement.

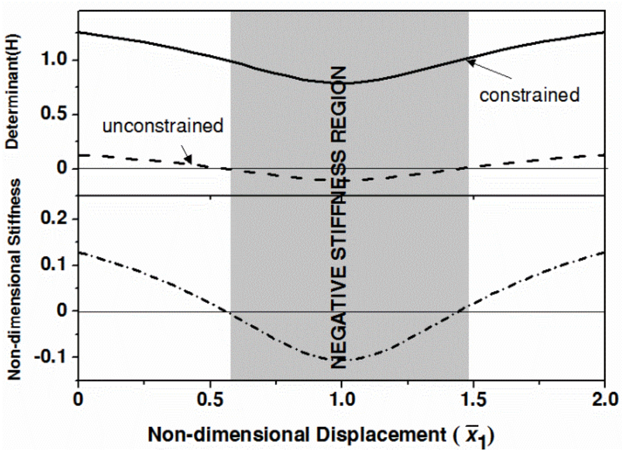

Fig. 5: Stability of unconstrained and constrained systems.

However, to take advantage of the analytical formulation by Lai and Lim [29], the non linear negative stiffness can be expressed as

$$\kappa_0 = \eta X + \varepsilon X^3 \,, \tag{11}$$

where the linear coefficient of elasticity of the spring is η and ε is assume as the cubic non-linearity part of the stiffness for the derivation but set as zero for calculation. Our model in Fig. 2 can now be represented with system connecting with linear and non-linear springs as we have in Fig. 6. The equation of motion about equilibrium position with cubic non-linearity gives

$$\begin{aligned} m_2\ddot{x}_2 + \kappa x_2 + \eta\,(x_2 - x_3) + \varepsilon\,(x_2 - x_3)^3 = 0\,, \\ m_3\ddot{x}_3 + \kappa x_3 + \eta\,(x_3 - x_2) + \varepsilon\,(x_3 - x_2)^3 = 0\,. \end{aligned} \tag{12}$$

Initial conditions

$$x_2\,(0) = X_2\,, \quad x_3\,(0) = X_3\,, \quad \dot{x}_2\,(0) = \dot{x}_3\,(0) = 0\,. \tag{13}$$

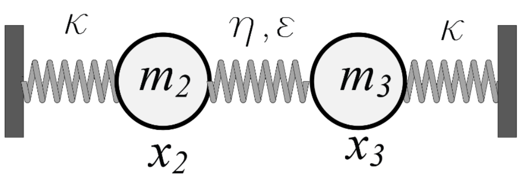

Fig. 6: Two mass system with non-linear negative stiffness springs.

Introducing new variables u and v as follows:

$$x_2 := u\,, \qquad x_3 - x_2 := v\,, \tag{14}$$

Eq. (12) can be transformed into

$$\ddot{u} + \gamma_1 u - \gamma_2 v - \gamma_3 v^3 = 0\,, \tag{15a}$$

$$\ddot{u} + \ddot{v} + \gamma_1 u + \gamma_1 v + \gamma_2 v + \gamma_3 v^3 = 0\,, \tag{15b}$$

where $\gamma_1 = \kappa/m$, $\gamma_2 = \eta/m$, $\gamma_3 = \varepsilon/m$ and $m_2 = m_3$. Solving for $\ddot{u}$ in Eq. (15a) and substituting in Eq. (15b) gives Duffing equation

$$\ddot{v} + \alpha v + \beta v^3 = 0\,. \tag{16}$$

For the analytical and numerical free vibration, it is assumed that

$$v(0) = x_3(0) - x_2(0) = X_3 - X_2 = V\,, \quad \dot{v}(0) = 0\,, \tag{17}$$

where $\alpha = \gamma_1 + 2\gamma_2$ and $\beta = 2\gamma_3$.

Equation (16) can be solved by different kinds of analytical approximation methods: perturbation, elliptic perturbation method, averaging procedure, Displacement of the two oscillators can be expressed as [29]

$$\begin{aligned} x_2(t) = {} & (X_2 + G_1 + H_1 + I_1 + J_1 + K_1 + L_1 + M_1 + N_1)\cos\sqrt{\gamma_1}t \\ & + G_2\cos(\omega_3 t) + H_2\cos(3\omega_3 t) + I_2\cos(5\omega_3 t) + J_2\cos(7\omega_3 t) \\ & + K_2\cos(9\omega_3 t) + L_2\cos(11\omega_3 t) + M_2\cos(13\omega_3 t) + N_2\cos(15\omega_3 t)\,, \end{aligned} \tag{18}$$

$$\begin{aligned} x_3(t) = {} & x_2(t) + (V + C1 + C2)\cos(\omega_3 t) \\ & + (C3 - C2 - C1)\cos(3\omega_3 t) - C3\cos(5\omega_3 t)\,. \end{aligned} \tag{19}$$

The expressions for all the variables in Eqns. (18), (19) are given in Ref. [29].

3.1 FREE VIBRATION

For free undamped vibration in the absence of driving force, 3 cases of initial conditions will be considered

- Case 1: $x_2(0) = 0.5$, $x_3(0) = 0$;
- Case 2: $x_2(0) = 0$, $x_3(0) = 0.4$; and
- Case 3: $x_2(0) = 0.5$, $x_3(0) = 0.4$.

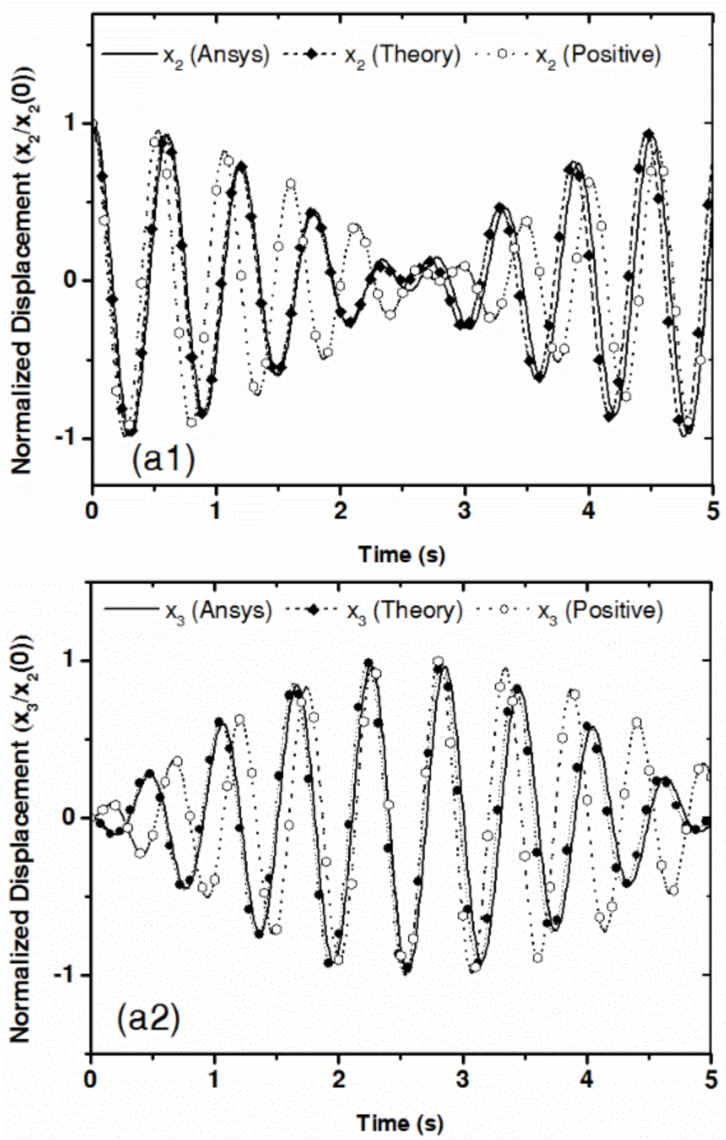

Fig. 7: Comparison of the numerical results with the analytical approximation at equilibrium point: (a) Case 1.

All simulation is done with $\dot{x}_2(0) = 0$, $\dot{x}_3(0) = 0$. In Figs. 7, 8 and 9 we have the same form of curves for the numerical (ANSYS) and theory (with zero non-linearity) which is in anti-phase with the positive stiffness (linear). The positive

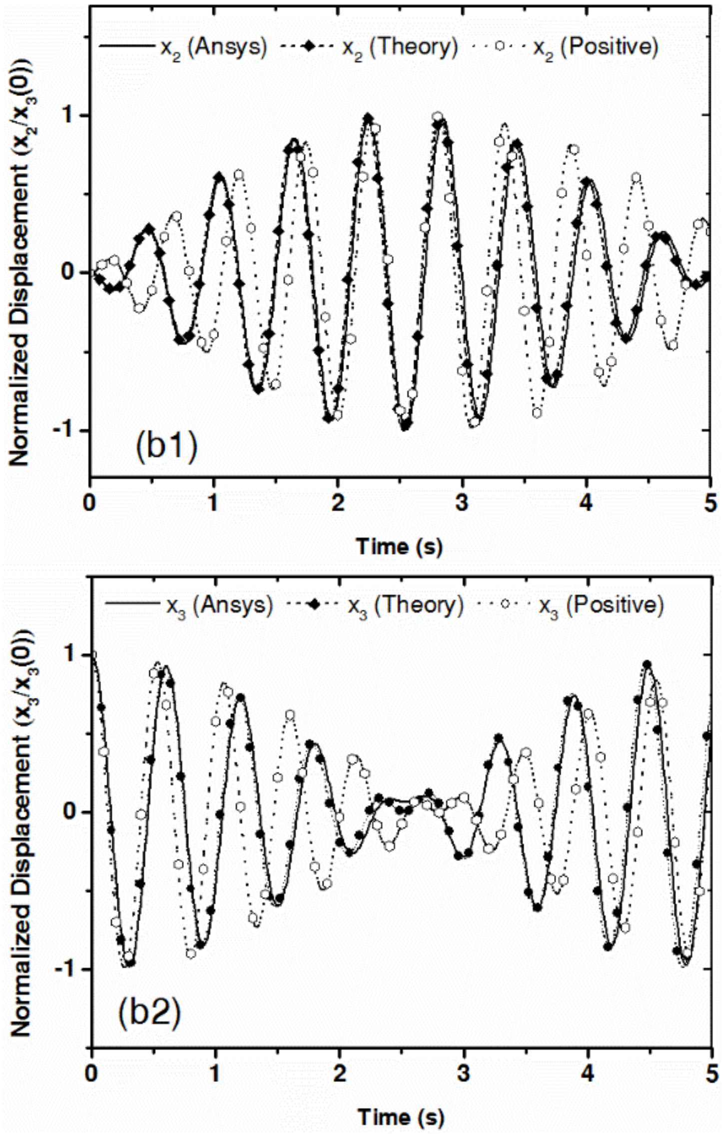

Fig. 8: Comparison of the numerical results with the analytical approximation at equilibrium point: (b) Case 2.

stiffness value is chosen as to show that there is transformation as oscillator 2 moves along the geometry. The anti-phase movement noticed in mass two in Fig. 7 and mass three in Fig. 8 corroborated the earlier submission that incorporating negative

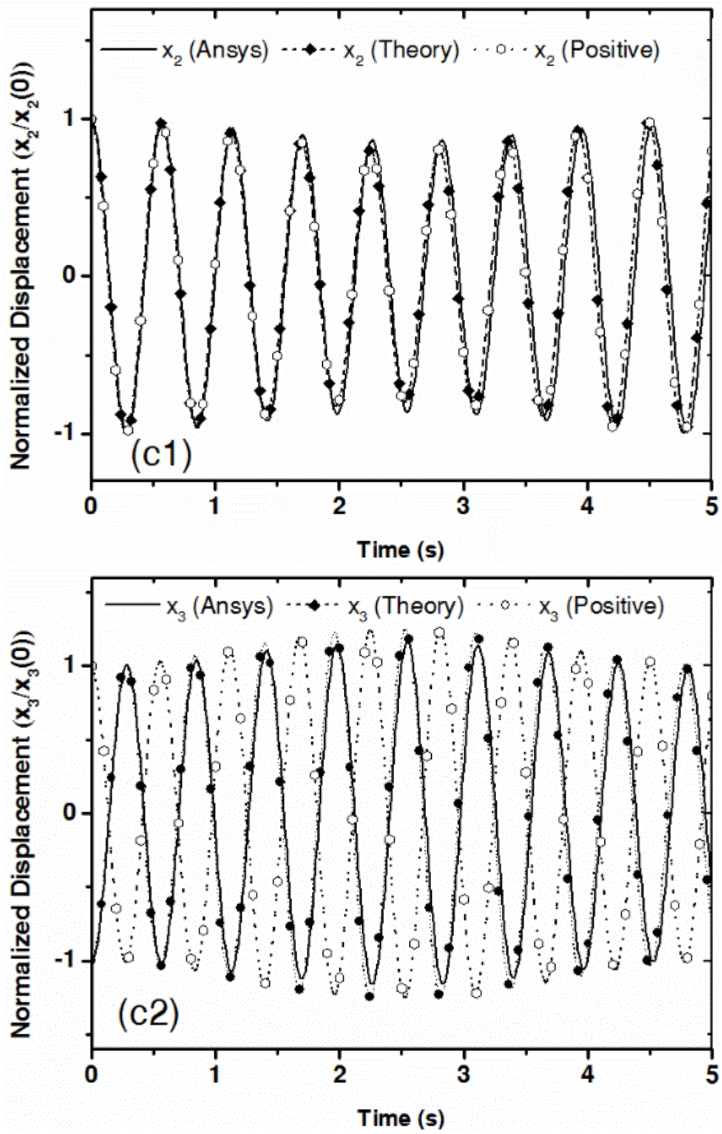

Fig. 9: Comparison of the numerical results with the analytical approximation at equilibrium point: (c) Case 3.

stiffness in positive matrix changes motion of one of the oscillator [10, 20]. The analytical approximation by NHB gives very matching patterns with the numerical solutions by ANSYS for the entire duration of time.

3.2 TRANSIENT RESPONSE

Furthermore, a short MATLAB code is written to test the response of the model under time-varying loads and the responses of the oscillators are plotted in Fig. 10. Numerical model from ANSYS agrees with the linear negative stiffness for a period of 4 and 3.5 seconds when the force is on mass two and mass three respectively. Applying the time varying force on mass two tends to agree better due to the rigid mass used to incline the springs, which tends to affect the trajectory of the member.

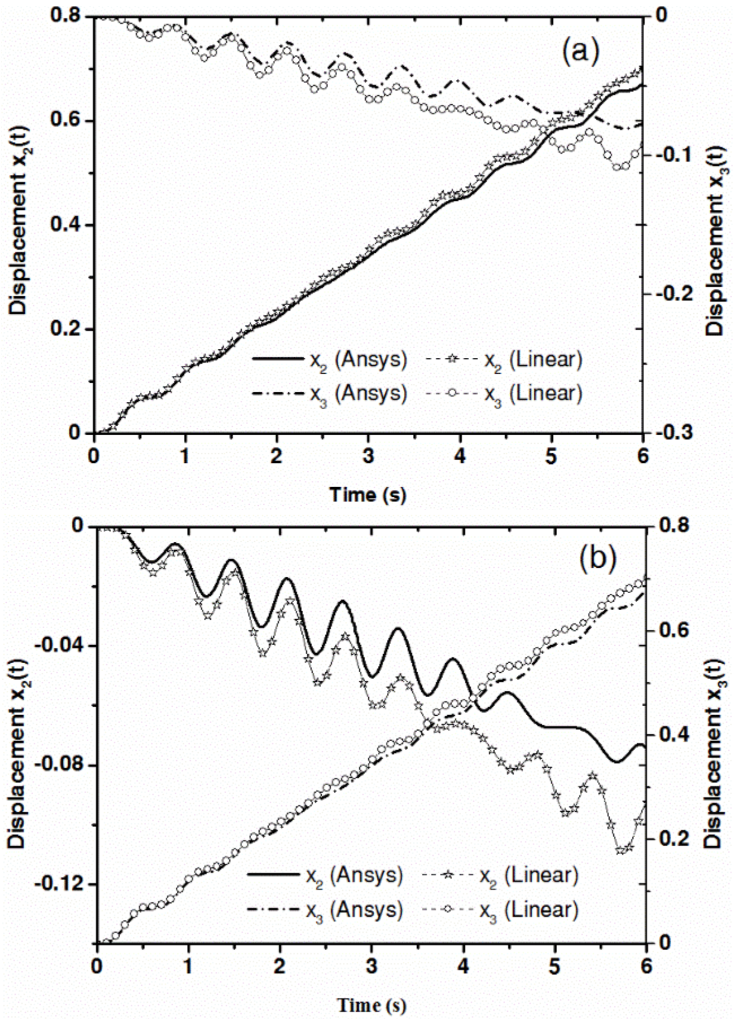

Fig. 10: Transient vibration of m_2 and m_3: a) with $F_{x_2}\left(t\right) = 0.1 * \left(t\right)$; and b) with $F_{x_3}\left(t\right) = 0.1 * \left(t\right)$.

4 Conclusions

In this paper, we have presented an alternative means of generating a stable linear negative stiffness through bi-stable element. The inclined spring and surrounding positive springs will determine whether we will have a stable negative stiffness or a jump from one stable point to another. The stability of the bi-stable element is achieved by constraining it within positive members. We showed numerically that chains of springs and masses connected in series containing spring with negative stiffness could still exhibit stable motion. For small amplitudes displacement, the bi-stable element behaves as a linear negative stiffness, which allows propagation of mechanical waves.

References

[1] M. Peyrard, M. Remoissenet (1982) Solitonlike excitations in a one-dimensional atomic chain with a nonlinear deformable substrate potential. *Physical Review B* **26**(6) 2886-2899.

[2] G. Puglisi, L. Truskinovsky (2000) Mechanics of a discrete chain with bi-stable elements. *Journal of the Mechanics and Physics of Solids* **48**(1) 1-27.

[3] M. Remoissenet, M. Peyrard (1979) Soliton brownian motion and impurities effects in one dimensional superionic conductors. *Solid State Communications* **31**(4) 229-232.

[4] M. Remoissenet (1986) Low-amplitude breather and envelope solitons in quasi-one-dimensional physical models. *Physical Review B* **33**(4) 2386-2392.

[5] J. Qiu, J. Lang, A. Slocum (2001) A centrally-clamped parallel-beam bistable MEMS mechanism, Technical Digest. *Proceedings of the IEEE Micro Electro Mechanical Systems (MEMS)* 353-356.

[6] S. Pellegrini, N. Tolou, M. Schenk, J. Herder (2013) Bistable vibration energy harvesters: A review. *Journal of Intelligent Material Systems and Structures* **24**(11) 1303-1312.

[7] R. Harne, M. Thota, K. Wang (2013) Bistable energy harvesting enhancement with an auxiliary linear oscillator. *Smart Materials and Structures. Eng.* **22**(12) 125028.

[8] T. Klatt, M. Haberman (2013) A nonlinear negative stiffness metamaterial unit cell and small-on-large multiscale material model. *Journal of Applied Physics* **114**(3) 033503.

[9] X. Fang, J. Wen, J. Yin, D. Yu (2017) Highly efficient continuous bistable nonlinear energy sink composed of a cantilever beam with partial constrained layer damping. *Nonlinear Dynamics* **87**(4) 2677-2695.

[10] E. Pasternak, A. Dyskin, G. Sevel (2014) Chains of oscillators with negative stiffness elements. *Journal of Sound and Vibration* **333**(24) 6676-6687.

[11] C.S. Wojnar, D.M. Kochmann (2014) A negative-stiffness phase in elastic composites can produce stable extreme effective dynamic but not static stiffness. *Philosophical Magazine* **94**(6) 532-555.

[12] D. KOCHMANN, W. DRUGAN (2009) Dynamic stability analysis of an elastic composite material having a negative-stiffness phase. *Journal of the Mechanics and Physics of Solids* **57**(7) 1122-1138.

[13] W. DRUGAN (2007) Elastic composite materials having a negative stiffness phase can be stable. *Physical Review Letters* **98**(5).

[14] X. HUANG, Y. CHEN, H. HUA, X. LIU, Z. ZHANGZ (2015) Shock isolation performance of a nonlinear isolator using Euler buckled beam as negative stiffness corrector: Theoretical and experimental study. *Journal of Sound and Vibration* **345** 178-196.

[15] I. KOVACIC, M. BRENNAN, T. WATERS (2008) A study of a nonlinear vibration isolator with a quasi-zero stiffness characteristic. *Journal of Sound and Vibration* **315**(3) 700-711.

[16] N. TOLOU, G. SMIT, A. NIKOOYAN, D. PLETTENBURG, J. HERDER (2012) Stiffness Compensation Mechanism for Body Powered Hand Prostheses with Cosmetic Covering. *Journal of Medical Devices* **6**(1) 011004.

[17] N. ATTARY, M. SYMANS, S. NAGARAJAIAH, A.M. REINHORN, M.C. CONSTANTINOU, A.A. SARLIS, D.T.R. PASALA, D. TAYLOR (2015) Performance Evaluation of Negative Stiffness Devices for Seismic Response Control of Bridge Structures via Experimental Shake Table Tests. *Journal of Earthquake Engineering* **19**(2) 249-276.

[18] T. JAGLINSKI, P. FRASCONE, B. MOORE, D. STONE, R. LAKES (2006) Internal friction due to negative stiffness in the indium-thallium martensitic phase transformation. *Philosophical Magazine* **86**(27) 4285-4303.

[19] L. DONG, D. STONE, R. LAKES (2011) Extreme anelastic responses in Zn80Al20 matrix composite materials containing BaTiO3 inclusion. *Scripta Materialia* **65**(4) 288-291.

[20] A. OYELADE, Z. WANG, G. HU (1981) Dynamics of 1D mass-spring system with a negative stiffness spring realized by magnets: Theoretical and experimental study. *Theoretical and Applied Mechanics Letters* **7**(1) 17-21.

[21] Y. ZHENG, X. ZHANG, Y. LUO, B. YAN, C. MA (2016) Design and experiment of a high-static–low-dynamic stiffness isolator using a negative stiffness magnetic spring. *Journal of Sound and Vibration* **360** 31-52.

[22] N. NADKARNI, C. DARAIO, D. KOCHMANN (2014) Dynamics of periodic mechanical structures containing bistable elastic elements: From elastic to solitary wave propagation. *Physical Review E - Statistical, Nonlinear, and Soft Matter Physics* **90**(2) 023204.

[23] J. YANG, Y. XIONG, J. XING (2013) Dynamics and power flow behaviour of a nonlinear vibration isolation system with a negative stiffness mechanism. *Journal of Sound and Vibration* **332**(1).

[24] E. RIKS (1979) An incremental approach to the solution of snapping and buckling problems. *International Journal of Solids and Structures* **15**(7) 529-551.

[25] M.A. CRISFIELD (1981) A fast incremental/iterative solution procedure that handles “snap-through”. *Computers and Structures* **13**(1-30 55-62.

[26] Y. WANG, R. LAKES (2004) Stable extremely-high-damping discrete viscoelastic systems due to negative stiffness elements. *Applied Physics Letters* **84**(22) 4451-4453.

[27] L. CVETICANIN (2003) Forced non-linear vibrations of a symmetrical two-mass system. *Journal of Sound and Vibration* **265**(2) 451-458.

[28] SHA. HASHEMI KACHAPI, RAO V. DUKKIPATI, S.GH. HASHEMI K., S.MEY. HASHEMI K., S.MEH. HASHEMI K., SK. HASHEMI K. (2010) Analysis of the nonlinear vibration of a two-mass-spring system with linear and nonlinear stiffness. *Nonlinear Analysis: Real World Applications* **11**(3) 1431-1441.

[29] S.K. LAI, C.W. LIM (2007) Nonlinear vibration of a two-mass system with nonlinear stiffnesses. *Nonlinear Dynamics* **49**(1-3) 233-249.